



3 4456 0515719 3

ORNL-4507  
UC-33 - Propulsion Systems and  
Energy Conversion

1

ORNL-4507  
UC-33 - Propulsion Systems and  
Energy Conversion

HELIUM RELEASE FROM  $^{238}\text{PuO}_2$  MICROSPHERES

Peter Angelini  
R. E. McHenry  
J. L. Scott  
W. S. Ernst, Jr.  
J. W. Prados

OAK RIDGE NATIONAL LABORATORY  
CENTRAL RESEARCH LIBRARY  
DOCUMENT COLLECTION  
**LIBRARY LOAN COPY**  
DO NOT TRANSFER TO ANOTHER PERSON  
If you wish someone else to see this  
document, send in name with document  
and the library will arrange a loan.

UCN-7969  
13-3-67



**OAK RIDGE NATIONAL LABORATORY**  
operated by  
**UNION CARBIDE CORPORATION**  
for the  
**U.S. ATOMIC ENERGY COMMISSION**

Printed in the United States of America. Available from Clearinghouse for Federal  
Scientific and Technical Information, National Bureau of Standards,  
U.S. Department of Commerce, Springfield, Virginia 22151  
Price: Printed Copy \$3.00; Microfiche \$0.65

LEGAL NOTICE

This report was prepared as an account of Government sponsored work. Neither the United States, nor the Commission, nor any person acting on behalf of the Commission:

- A. Makes any warranty or representation, expressed or implied, with respect to the accuracy, completeness, or usefulness of the information contained in this report, or that the use of any information, apparatus, method, or process disclosed in this report may not infringe privately owned rights; or
- B. Assumes any liabilities with respect to the use of, or for damages resulting from the use of any information, apparatus, method, or process disclosed in this report.

As used in the above, "person acting on behalf of the Commission" includes any employee or contractor of the Commission, or employee of such contractor, to the extent that such employee or contractor of the Commission, or employee of such contractor prepares, disseminates, or provides access to, any information pursuant to his employment or contract with the Commission, or his employment with such contractor.

Contract No. W-7405-eng-26

HELIUM RELEASE FROM  $^{238}\text{PuO}_2$  MICROSPHERES

Peter Angelini and R. E. McHenry

Isotopes Division

J. L. Scott and W. S. Ernst, Jr.

Metals and Ceramics Division

J. W. Prados

Consultant, University of Tennessee

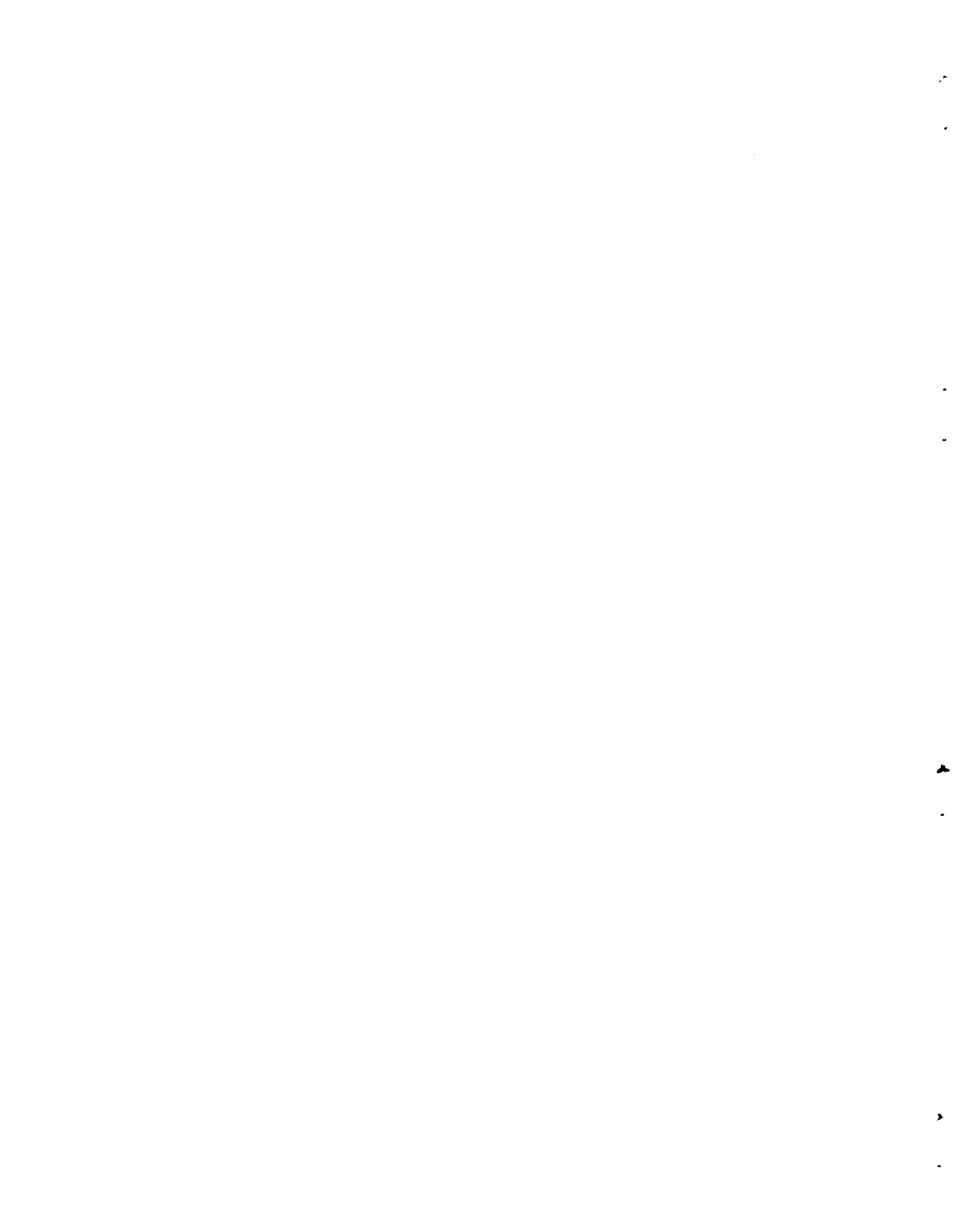
MARCH 1970

OAK RIDGE NATIONAL LABORATORY  
Oak Ridge, Tennessee  
operated by  
UNION CARBIDE CORPORATION  
for the  
U. S. ATOMIC ENERGY COMMISSION

LOCKHEED MARTIN ENERGY RESEARCH LIBRARIES



3 4456 0515719 3



HELIUM RELEASE FROM  $^{238}\text{PuO}_2$  MICROSPHERES

Peter Angelini  
R. E. McHenry  
J. L. Scott  
W. S. Ernst, Jr.  
J. W. Prados

## ABSTRACT

The release of helium from plasma-melted  $^{238}\text{PuO}_2$  microspheres was investigated under two experimental conditions: isothermal steady-state release at 100 to 1300°C and release during and following a transient-temperature rise from ambient to a constant final value ranging from 900 to 1900°C, with heatup time of 2 to 5 min. Release characteristics could be approximately described by diffusion models; however, different correlations of diffusion parameters were required for the two types of experiments.

The transient-heating experiments yielded two particularly significant results: helium release was complete above 1300°C within 10 min (less at higher temperatures) and mechanical degradation of the microspheres was negligible.

A reasonable explanation of the mechanism for the steady-state results is proposed. The mechanism of helium release under transient conditions is unclear, but appears to differ significantly from that at steady state.

---

  
INTRODUCTION

Several isotopic-power fuels under development<sup>1</sup> utilize the decay energy of one of the alpha-emitting nuclides  $^{238}\text{Pu}$ ,  $^{244}\text{Cm}$ , or  $^{210}\text{Po}$ . The alpha decay of these substances continuously generates helium in fuel bodies containing them. The design of safe and efficient isotopic-power fuels will require a knowledge of the characteristics of helium release from such bodies.

At present little is known of the motion of helium in actinide oxides. One might conjecture that the process is analogous to the motion of fission-product xenon and krypton in reactor fuel. However, in spite of intensive research conducted on the latter problem over the past 20 years, neither an accurate mathematical description nor an accepted

explanation of the mechanism exists for the motion of fission-product gases in the most common of reactor fuels,  $UO_2$ . Detailed discussions of this problem have appeared in recent literature.<sup>2-6</sup>

The present study was undertaken in an effort to provide helium-release information of use to designers of isotopic-power supplies using plasma-melted  $^{238}PuO_2$  microspheres as the heat source. Experimental measurements of helium release from such materials were for two situations: isothermal steady-state release of helium at 100 to 1300°C and release during and following a transient-temperature rise from ambient to a constant final value ranging from 900 to 1900°C with heatup times of 2 to 5 min. The steady-state experiments represent the condition of isotopic fuels in storage or during normal operation of a power source; the rapid heatup experiments represent conditions that might be encountered during atmospheric re-entry of a space vehicle or during a launch-pad fire. Experimental results were correlated in terms of diffusion models which allow prediction of helium-release rates from plasma-melted  $^{238}PuO_2$  microspheres under conditions approximating those of the experiments. Some conjectures on helium-release mechanisms were also proposed, based on the experimental release results and metallographic examination of the microspheres.

#### MATHEMATICAL MODELS FOR RELEASE

As previously noted, no definitive information exists on the mechanism of release of helium or other inert gases from actinide oxides. In the light of experience with reactor fuels, it is unrealistic to assume that a classical diffusion mechanism will provide a full description of the observed release behavior. However, the mathematics of diffusion often permit the representation of release data in terms of relatively simple equations with a small number of arbitrary parameters. Hence a diffusion-model approach was employed in the present work, and mathematical relations describing the release were derived under the following assumptions:

1. The basic helium-releasing unit is a sphere of effective radius,  $a$ . This radius will probably be significantly smaller than the actual microsphere radius because of open porosity, grain boundaries, etc. in the microspheres.
2. The concentration of helium at the external surface of each releasing unit is zero. This assumption is believed to be justified by the extremely low solubility of inert gases in actinide oxides.<sup>7</sup>
3. The helium motion can be described by Fick's law, with an effective diffusion coefficient,  $D$ , within each releasing unit. This coefficient is independent of position (but can vary with time in the transient-heating experiments).

Additional assumptions for specific experiments are noted.

### Steady-State Experiments

In the steady-state release experiments it was assumed that generation of helium within the material occurred at a rate,  $P$  ( $\text{cm}^3$  of gas)/( $\text{cm}^3$  of solid)(sec), independent of time and position. At steady state the release rate of helium will equal the generation rate and under the foregoing assumptions the concentration distribution of helium within a releasing spherical unit is given by<sup>7</sup>

$$c(r) = \frac{P}{6D} (a^2 - r^2) , \quad (1)$$

where

$$\begin{aligned} c(r) &= \text{concentration of helium at radius } r, \text{ cm}^3/\text{cm}^3, \\ a &= \text{effective radius of releasing unit, cm,} \\ D &= \text{effective diffusion coefficient, cm}^2/\text{sec.} \end{aligned}$$

The average concentration within the sphere,  $C_{av}$ , may then be calculated as<sup>8</sup>

$$C_{av} = \frac{P}{15D'}, \quad (2)$$

where  $D' = D/a^2$ , the effective diffusion-release parameter,  $\text{sec}^{-1}$ . Experimentally, the sample is maintained at the required temperature in vacuum until the measured helium-release rate equals the known generation rate. The average helium concentration is then determined by melting and degassing the sample, and an effective diffusion parameter,  $D'$ , can be calculated directly from Eq. (2).

### Transient-Heating Experiments

The following additional assumptions were invoked in developing relations to describe the transient-heating experiments:

1. No release of helium occurs up to some time,  $t_0$ , measured from the start of the heatup period; then release obeys the usual diffusion laws.
2. The concentration of diffusing species is uniform at time  $t_0$ . (The method could be applied as well if the initial concentration profile were nonuniform but known.)
3. The experimental duration is short enough and initial helium inventories high enough that the small continuous internal generation of helium may be neglected.

Under these assumptions the theoretical fraction of helium released,  $f$  (amount released)/(amount initially present), at any time,  $t$ , is given by<sup>9</sup>

$$f = 0 \quad t \leq t_0 \quad (3a)$$

$$f = 1 - \frac{6}{\pi^2} \sum_{n=1}^{\infty} \frac{1}{n^2} \exp(-n^2\pi^2\tau) \quad t \geq t_0 \quad (3b)$$

where  $\tau$  is defined by

$$\tau = \int_{t_0}^t D' dt. \quad (4)$$

For values of  $f$  below 0.77 ( $\tau \leq 0.15$ ), it can be shown that<sup>10</sup>

$$f \approx 6\sqrt{\frac{\tau}{\pi}} - 3\tau, \quad (5)$$

while for  $f$  above 0.77 ( $\tau \geq 0.15$ ),

$$f \approx 1 - \frac{6}{\pi^2} \exp(-\pi^2\tau). \quad (6)$$

The use of these equations in data analysis is discussed in a later section.

## EXPERIMENTAL

### Material

The  $^{238}\text{PuO}_2$  microspheres that were examined in these studies were prepared from Mound Laboratory by a plasma-melting technique and were selected from typical material used to fuel radioisotopic heat sources. Two samples of  $^{238}\text{PuO}_2$  microspheres in two size ranges were supplied. The two samples were designated SN370/376 and Dart I, and their compositions and densities were given as 80.25 wt %  $^{238}\text{PuO}_2$  and 10.45 g/cm<sup>3</sup> and 80.38 wt %  $^{238}\text{PuO}_2$  and 10.00 g/cm<sup>3</sup>, respectively. The analysis date for both samples was January 1967. The size ranges for the samples were 177- to 210- $\mu\text{m}$  diameter and 74- to 88- $\mu\text{m}$  diameter.

The SN370/376 fuel was processed in January 1967 and then subjected intermittently to temperatures of up to 800°C before the helium inventory was measured at ORNL on April 10, 1968. Dart I fuel was also processed in January 1967 and then subjected intermittently to temperatures of up to 1200°C until May 4, 1967, when it was subjected to temperatures of 1200°C until April 4, 1968. On April 4, 1968, the temperatures were changed to ambient. The helium inventory was measured at ORNL on June 6, 1968.

## Apparatus

### Rapid-Heat Furnace

The furnace in which the microspheres were heated rapidly is shown in Fig. 1. This furnace, which can be operated at  $\sim 2000^{\circ}\text{C}$  indefinitely, is a water-cooled vacuum type with a tantalum resistance-heating element. A molybdenum sample tube contains the capsule in which the microspheres are loaded and projects downward into the hot zone of the furnace through a water-cooled seal. Windows and black-body holes are provided for temperature measurements. The furnace bonnet is attached to the furnace base with a vacuum seal, permitting easy access for furnace maintenance. A mechanical pump maintains the furnace vacuum, and power for the furnace is supplied by a variable voltage (0 to 42 V, dc) 600-Amp capacity rectifier. The power supply was motorized to program the required rate of temperature rise.

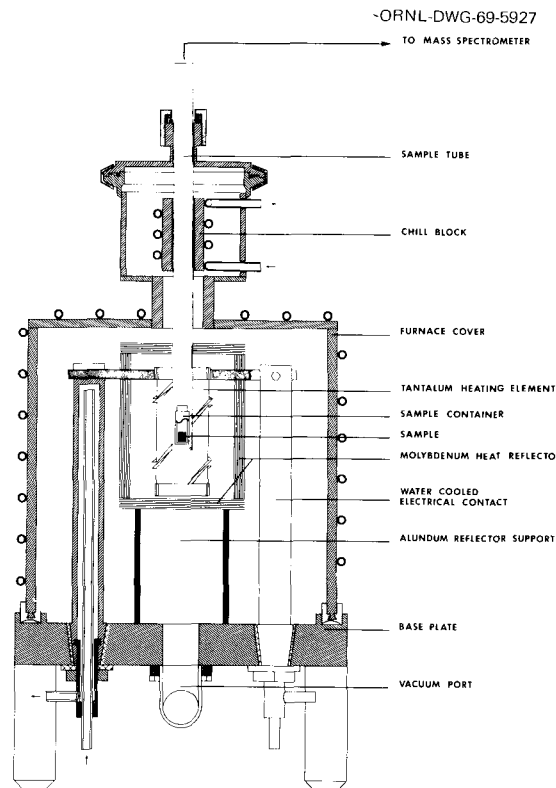


Fig. 1. Vacuum Furnace.

### Steady-State Furnace

The furnace used for measurement of the helium-release rates under steady-state conditions had a platinum-wire-wound resistance element. Power was supplied by a variable ac transformer. The furnace, which was usable up to  $1600^{\circ}\text{C}$ , could be operated with either an argon or a vacuum atmosphere in contact with the  $^{238}\text{PuO}_2$ .

### Helium Detector

The helium-release rates from  $^{238}\text{PuO}_2$  were measured with a National Research Corporation Model 925 mass-spectrometer leak detector. The sensitivity range of the mass spectrometer is  $2 \times 10^{-11}$  to  $6 \times 10^{-5}$   $\text{cm}^3$  of helium per second. The span range of the instrument for a given set of adjustments (and calibration) is approximately four decades. The leak detector was calibrated by using helium leaks standardized by the Y-12 Plant. The signal from the leak detector was plotted by a suitable recorder.

### Pyrometers

The temperature of the rapid-heat furnace was obtained with a micro-optical pyrometer manufactured by Pyrometer Instrument Company.

## Glove Box

The furnaces in which the  $^{238}\text{PuO}_2$  microspheres were heated were contained inside clear plastic glove boxes. The exhaust from the glove boxes was connected to the building exhaust system through absolute filters and the exhaust system maintained the atmosphere of the glove boxes at a negative pressure of 0.5-in. water (gage).

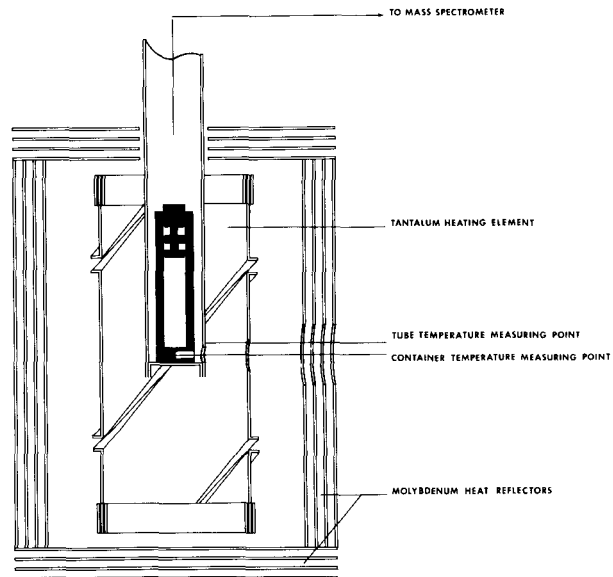
The lines from the furnaces to the vacuum pumps and/or helium detector which were outside the glove boxes contained filters to prevent possible flow of radioactive material. Safety devices were provided to remove power from the furnaces in the event cooling water was lost or water lines were ruptured in the glove boxes.

## Procedure

### Temperature Measurement

ORNL-DWG 69-6253

During the rapid-heat experiments the temperature of the  $^{238}\text{PuO}_2$  microspheres could not be observed directly. Temperature measurements of the sample tube recorded during the runs were known to contain errors due to lack of black-body conditions, lag of the sample container temperature behind that of the sample tube because of heat transfer during heatup, and absorption of energy by windows. Calibration runs were made for each temperature ramp employed, and the temperature of a black-body hole in the sample container was measured simultaneously with that of the sample tube. During the calibration runs a hole was present in a dummy sample (see Fig. 2). Corrections were made, where required, by calibrating the pyrometer with pure material of known melting points (gold,  $\text{Al}_2\text{O}_3$ , etc.). The temperature of the furnace used in the steady-state determinations was measured with Pt-PtRh thermocouples.



LOCATIONS OF TEMPERATURE MEASUREMENTS

Fig. 2.  $^{238}\text{PuO}_2$  Sample Temperature Measurement.

### Transient-Heating Experiments

Prior to a transient-heating experiment the power supply controls were adjusted to program the furnace to the required temperature in the required time, and the furnace was degassed at 1800 to 2000°C. The quantity of  $^{238}\text{PuO}_2$  for each experiment was chosen to produce helium-release rates near the upper limits of the sensitivity of the detector (e.g., 50 mg of  $^{238}\text{PuO}_2$  at 900°C and 5 mg of  $^{238}\text{PuO}_2$  at 1900°C).

The microsphere sample was placed in the sample container, designed to minimize any transfer of  $^{238}\text{PuO}_2$  from the container either mechanically or by vaporization, and the container was inserted into the sample tube of the furnace, which was connected to the helium detector. The assembled apparatus was thoroughly degassed by pumping, the leak detector was calibrated, and power to the furnace was turned on.

The temperature was recorded periodically and the helium-release rate continuously until the release rate decreased to the lower sensitivity limits of the detector. The total helium release as a function of time was obtained by integration of the release-rate curve.

#### Steady-State Experiments

The quantity of  $^{238}\text{PuO}_2$  samples used during a determination of the diffusion parameter at steady state was such that the steady-state helium concentration in the sample was well within the sensitivity of the detector. The helium-release rates at steady state were, of course, equal to the production rate for the sample size used. (The helium production rate was  $1.65 \times 10^{-8}$  cm<sup>3</sup> of helium per sec per g of  $\text{PuO}_2$ ). The sample size was usually 200 to 300 mg. The sample of  $^{238}\text{PuO}_2$  was brought to temperature in the furnace previously described and kept at a steady temperature in either a vacuum or an argon atmosphere until the helium-release rate closely approached the generation rate. The release rate was monitored periodically. When the sample reached steady state, it was quickly transferred to the rapid-heat furnace and the helium inventory in the sample was determined.

#### Helium Inventory Determination

The helium concentration in the  $^{238}\text{PuO}_2$  that was rapidly heated to high temperature was determined in the rapid-heat furnace, which was also used to determine the concentration of helium in samples that had been brought to steady state. The temperature of the sample in the furnace was increased at the highest rate that would allow the release rate to remain on the scale of the detector. The temperature was increased to 1900°C. Experiments on melting samples of  $\text{PuO}_2$  as a eutectic (133 mg of  $\text{Al}_2\text{O}_3$ , 162 mg of  $\text{BeO}$ , 350 mg of  $\text{PuO}_2$ ) indicated that the helium release was essentially complete at 1900°C.

### RESULTS

#### Steady-State Diffusion Parameters

Effective diffusion parameters,  $D'$ , determined from 14 steady-state release experiments at 100 to 1300°C are shown in Table 1. Two determinations were made in an argon atmosphere. The diffusion parameters were calculated from the helium production rate,  $P$ , and the average helium concentration,  $C_{\text{av}}$ , using Eq. (2). The calculated diffusion parameters did not depend significantly on microsphere radius, indicating that the effective helium-releasing units were considerably smaller than the microspheres themselves.

Table 1. Apparent Helium Diffusion Parameters Based on Determinations Under Steady-State Helium Release Conditions

Temperature °C	Temperature 1/T, °K	Atmospheric Composition	Time <sup>a</sup> at Temp, hr	D', sec <sup>-1</sup>
<u>SN370/376 Fuel (177 to 210 μm)</u>				
800	$9.3 \times 10^{-4}$	Vacuum	1136	$4.78 \times 10^{-9}$
1000	$7.85 \times 10^{-4}$	Vacuum	480	$1.31 \times 10^{-8}$
1300	$6.35 \times 10^{-4}$	Vacuum	145	$6.31 \times 10^{-7}$
<u>Dart I Fuel (177 to 210 μm)</u>				
800	$9.3 \times 10^{-4}$	Vacuum	1136	$3.2 \times 10^{-9}$
1000	$7.85 \times 10^{-4}$	Vacuum	600	$1.72 \times 10^{-8}$
1100	$7.3 \times 10^{-4}$	Vacuum	552	$2.52 \times 10^{-8}$
1100	$7.3 \times 10^{-4}$	Argon <sup>b</sup>	552	$4.03 \times 10^{-8}$
1300	$6.35 \times 10^{-4}$	Vacuum	52	$5.91 \times 10^{-7}$
1320	$6.28 \times 10^{-4}$	Vacuum	20	$7.05 \times 10^{-7}$
1400	$5.98 \times 10^{-4}$	Vacuum	19	$3.9 \times 10^{-6}$
1500	$5.63 \times 10^{-4}$	Vacuum	21	$1.02 \times 10^{-5}$
1560	$5.45 \times 10^{-4}$	Vacuum	6	$3.57 \times 10^{-5}$
<u>Dart I Fuel (74 to 88 μm)</u>				
1000	$7.85 \times 10^{-4}$	Argon <sup>c</sup>	1776	$2.17 \times 10^{-8}$
1000	$7.85 \times 10^{-4}$	Vacuum	1776	$3.65 \times 10^{-8}$

<sup>a</sup>Not time to steady state, which is less than these values.

<sup>b</sup>0.2 atm.

<sup>c</sup>1 atm.

The data in Table 1 are shown as an Arrhenius plot in Fig. 3. The curve as drawn could be explained by the simultaneous and independent release processes with activation energies of 77.1 and 17.9 kcal/mole, respectively.

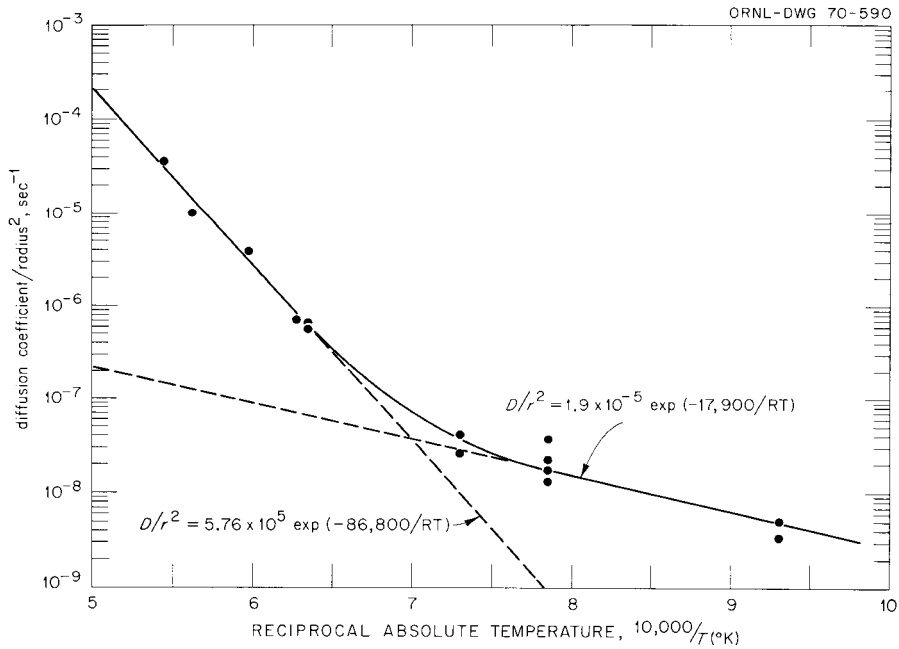


Fig. 3. Correlation of Diffusion Parameter, D', with Temperature for Steady-State Experiments.

### Helium Inventory in Samples

The helium concentrations in the  $^{238}\text{PuO}_2$  microspheres, determined soon after receipt at ORNL and again at a later date, are given in Table 2. During the interval between determinations, the SN370/376 (177 to 210  $\mu\text{m}$ ) fuel retained 65% of the helium generated, while Dart I fuel retained 64%.

Table 2. Helium Inventory in SN370/376 and Dart I  $^{238}\text{PuO}_2$  Fuels

Date	Fuel Designation	Size, $\mu\text{m}$	He Inventory, $\text{cm}^3/\text{g}$ of fuel
4-1-68	SN370/376	177-210	0.228
4-10-68	SN370/376	74-88	0.238
6-6-68	Dart I	74-88	0.127
6-6-68	Dart I	177-210	0.101
10-15-68	SN370/376	177-210	0.44
10-17-68	SN370/376	177-210	0.39
10-15-68	Dart I	177-210	0.24
10-18-68	Dart I	177-210	0.20

### Transient-Heating Experiments

Twenty runs were carried out in which  $^{238}\text{PuO}_2$  microspheres were heated at a rate of  $\sim 5.5^\circ\text{C}/\text{sec}$  from ambient to a final temperature in the range of 900 to  $1900^\circ\text{C}$  and held at this temperature until helium release fell below the limit of detection of the apparatus. Typical curves of temperature, release rate, and release fraction as functions of time are shown in Fig. 4 (final temperature  $1100^\circ\text{C}$ ) and Fig. 5 (final temperature  $1700^\circ\text{C}$ ).

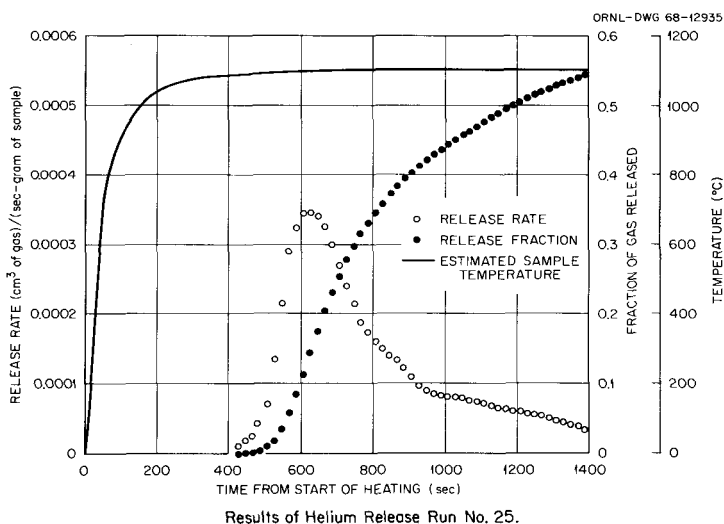


Fig. 4. Experimental Results for Transient Heating to  $1100^\circ\text{C}$  in  $\sim 200$  sec.

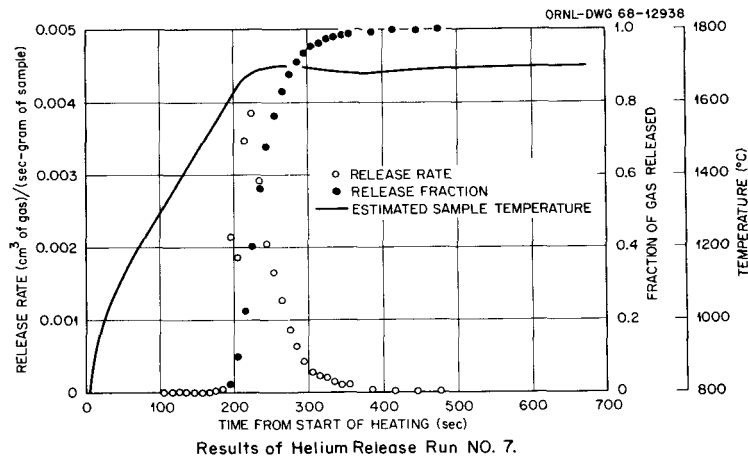


Fig. 5. Experimental Results on Transient Heating to 1700°C in ~250 sec.

The procedure employed in analyzing the experimental values of the release fraction,  $f$ , as a function of time,  $t$ , is outlined in the following steps:

1. From Eq.'s (3), (5), or (6) calculate the value of  $\tau$  corresponding to each experimentally determined  $f$ .
2. From experimental data and step 1 find the value of  $\tau$  corresponding to each time,  $t$ .
3. Plot a curve of  $\tau$  vs  $t$ ; the slope at any time is the value of the diffusion parameter,  $D'$ , at that time, since from Eq. (4)

$$D' = \frac{d\tau}{dt}. \quad (7)$$

For most of the transient-heating experiments, the plot of  $\tau$  vs  $t$  lies along the abscissa out to some given time, then rises almost linearly until well over 90% of the helium has been released. The slope of the linear portion is taken as  $D'$ , while the intercept of a line of this slope with the abscissas is taken as  $t_0$ . It was found in the present experiments that  $t_0$  is well approximated by the time at which 2% of the helium is released ( $f = 0.02$ ).

Such a plot is shown in Fig. 6 for the run illustrated in Fig. 5. From the slope of the linear portion of the plot a  $D'$  value of  $3.0 \times 10^{-3} \text{ sec}^{-1}$  was estimated, while the horizontal intercept of this line gave a  $t_0$  value of 220 sec. In Fig. 7 a curve of release fraction vs time calculated from this pair of  $D'$  and  $t_0$  values is compared with the experimental results. The results of all 20 runs, including the  $D'$  and  $t_0$  values calculated in this manner, are summarized in Table 3. It is significant to note that for final temperatures of 1300°C and above, all helium was released from the sample in a few minutes. Times to release 90% of the gas were somewhat erratic at 1300°C, but at higher temperatures they were significantly less than 10 min.

The  $D'$  and  $t_0$  values from all transient-heating experiments were correlated as functions of temperature. Arrhenius plots were constructed as shown in Figs. 8 and 9, and least-squares straight lines through the points yielded the following correlating equations:

$$\frac{1}{t_0} = 0.0717 \exp\left(-\frac{10,200}{RT}\right) \text{ sec}^{-1} \quad (8)$$

$$D' = 198 \exp\left(-\frac{41,800}{RT}\right) \text{ sec}^{-1} \quad (9)$$

where  $T$  is the final temperature,  $^{\circ}\text{K}$ ;  $900 \leq T \leq 1900^{\circ}\text{K}$ . Although these correlations are not as precise as one might wish, they do provide a means of estimating helium-release characteristics from  $^{238}\text{PuO}_2$  microspheres under rapid transient-heating conditions.

Table 3. Summary of Results for Helium Release from  $^{238}\text{PuO}_2$  Microspheres in Transient-Heating Experiments

Run No.	Final Temp., $^{\circ}\text{C}$	Time to Attain Final Temp., sec	Effective <sup>a</sup> $D'$ for Run, $\text{sec}^{-1}$	Effective <sup>a</sup> $t_0$ , sec	Final Release Fraction	Time to Release 90% of Final Fraction, sec
<u>370 Fuel (177 to 210 <math>\mu\text{m}</math>)</u>						
31	900	165	$4.4 \times 10^{-9}$	960	0.012	3210
25	1100	200	$5.8 \times 10^{-5}$	625	0.572	1240
26	1100	380	$2.5 \times 10^{-5}$	825	0.349	1200
9	1300	300	$9.0 \times 10^{-4}$	315	1.087	525
17	1500	270	$1.5 \times 10^{-3}$	210	1.025	335
24	1500	360	$3.0 \times 10^{-3}$	235	0.872	295
7	1700	250	$3.0 \times 10^{-3}$	220	0.940	280
16	1900	290	$4.8 \times 10^{-3}$	165	0.928	205
<u>370 Fuel (74 to 88 <math>\mu\text{m}</math>)</u>						
19	1300	350	$2.8 \times 10^{-4}$	300	0.988	1200
21	1500	215	$1.1 \times 10^{-3}$	270	0.484 <sup>b</sup>	375
22	1700	185	$2.3 \times 10^{-3}$	200	1.098	270
<u>Dart Fuel (177 to 210 <math>\mu\text{m}</math>)</u>						
38	1100	155	$7.8 \times 10^{-5}$	625	0.543	870
37	1300	320	$5.0 \times 10^{-4}$	375	1.096	1040
36	1500	270	$2.0 \times 10^{-3}$	195	1.078	290
30	1700	250	$2.3 \times 10^{-3}$	230	0.821 <sup>b</sup>	310
<u>Dart Fuel (74 to 88 <math>\mu\text{m}</math>)</u>						
46	900	125	$8.2 \times 10^{-7}$	1030	0.125	3000
52	1100	150	$3.0 \times 10^{-5}$	750	0.763	295
40	1300	300	$1.1 \times 10^{-3}$	325	0.649 <sup>b</sup>	475
44	1500	290	$1.6 \times 10^{-3}$	265	0.697 <sup>b</sup>	395
45	1700	180	$5.2 \times 10^{-3}$	180	0.602 <sup>b</sup>	215

<sup>a</sup>Values give good representation of data up to about 90% of final release fraction.

<sup>b</sup>Values believed to be  $1.0 \pm 0.1$ ; instrument calibration changed during experiment.

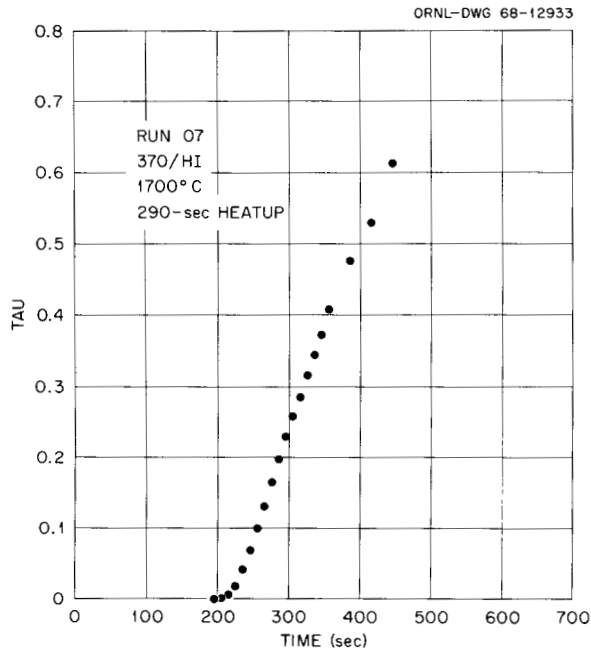


Fig. 6. Plot of  $\tau$  vs Time for Experimental Results Shown in Fig. 4.

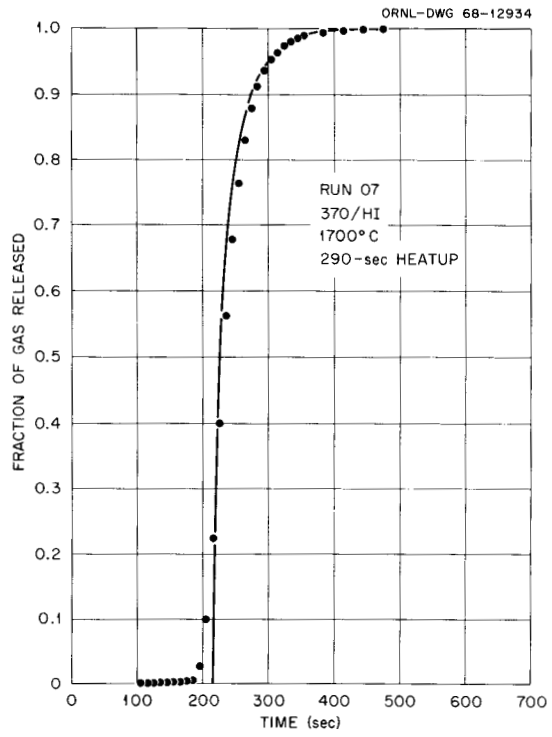


Fig. 7. Comparison of Measured and Calculated Release Fractions for Experimental Results Shown in Fig. 4.

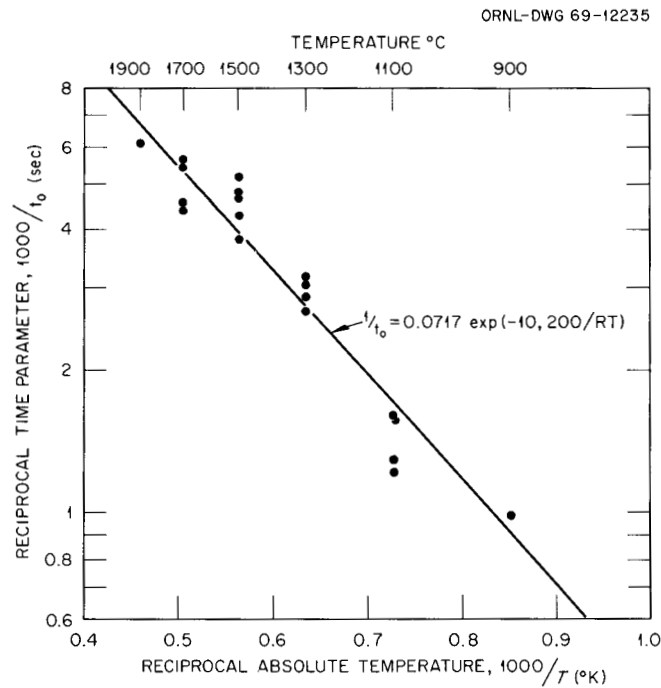


Fig. 8. Correlation of Time Parameter,  $t_0$ , with Temperature for Transient-Heating Experiments.

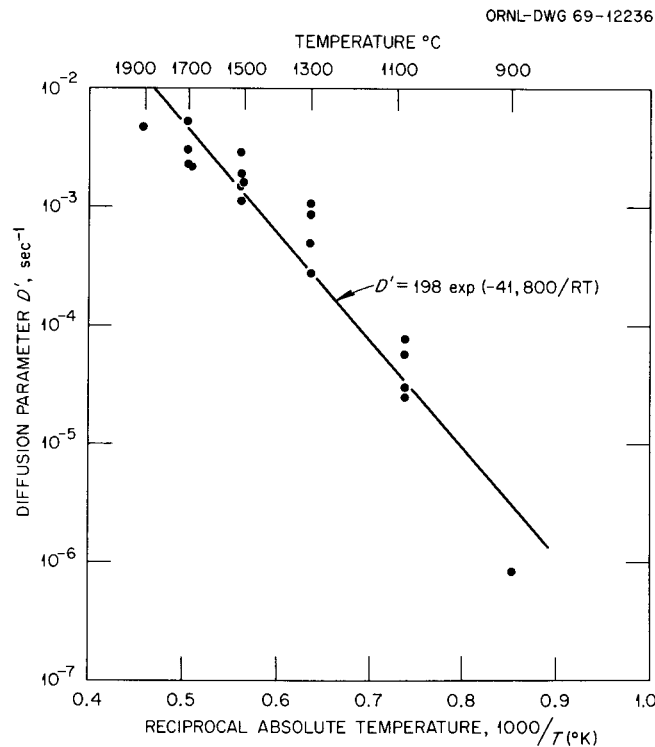


Fig. 9. Correlation of Diffusion Parameter,  $D'$ , with Temperature for Transient-Heating Experiments.

A qualitative, but highly significant, observation during the transient-heating experiments was the almost complete absence of particle fragmentation or degradation, in spite of the rapid thermal transients and gas release.

#### METALLOGRAPHY OF FUELS

Metallographic examination of microspheres composed of  $^{238}\text{PuO}_2$  showed that nothing catastrophic occurs as a result of rapidly heating them in vacuum. In the higher temperature experiments there is some evidence that a small fraction of the microspheres blow apart. Quantitative metallography was not possible because of the limited number of samples and the difficulty in mounting the particles.

In the rapid-heat experiments only about 5 mg of microspheres could be heated because of the sensitivity of the gas detector. For metallography about four times this amount was needed and necessitated separate heat treatments of the larger amounts. In preparing the metallographic specimens, the heating schedules were identical to those obtained during the rapid-heat experiments. During these preparatory runs it was not possible to monitor the actual gas released; therefore, it is necessary to assume that the larger samples used for metallography behaved similarly to the smaller samples used to obtain quantitative release data.

The major problem in making the metallographic mounts was that the epoxy mounting material would only partially adhere to the  $^{238}\text{PuO}_2$ . Therefore, during grinding and polishing of the mounted specimens, a number of the particles fell out of the mount. The mounts also deteriorated with age because gas accumulated in the boundary between the particle and epoxy. In spite of these difficulties, the metallographic evidence is apparent and supports the view that nothing serious results from rapid heating of the microspheres.

The metallographic evidence consists of a series of photographs taken of the fuel before and after heat treating at several temperatures. Cross sections of typical SN370/376 and Dart I fuels in the as-received condition are shown in Figs. 10-14. In Figs. 10 and 11 the large central void is typical of both the SN370/376 and the Dart I fuels. Figure 12 shows a particle having a relatively high bulk density. Particles of this kind probably made up <10% of the total. Figures 13 and 14 are characterized by larger voids and second-phase inclusions. Large distributed voids of the type shown in Fig. 15 were common in the Dart I fuel. Gas bubbles were not evident in these cold specimens.

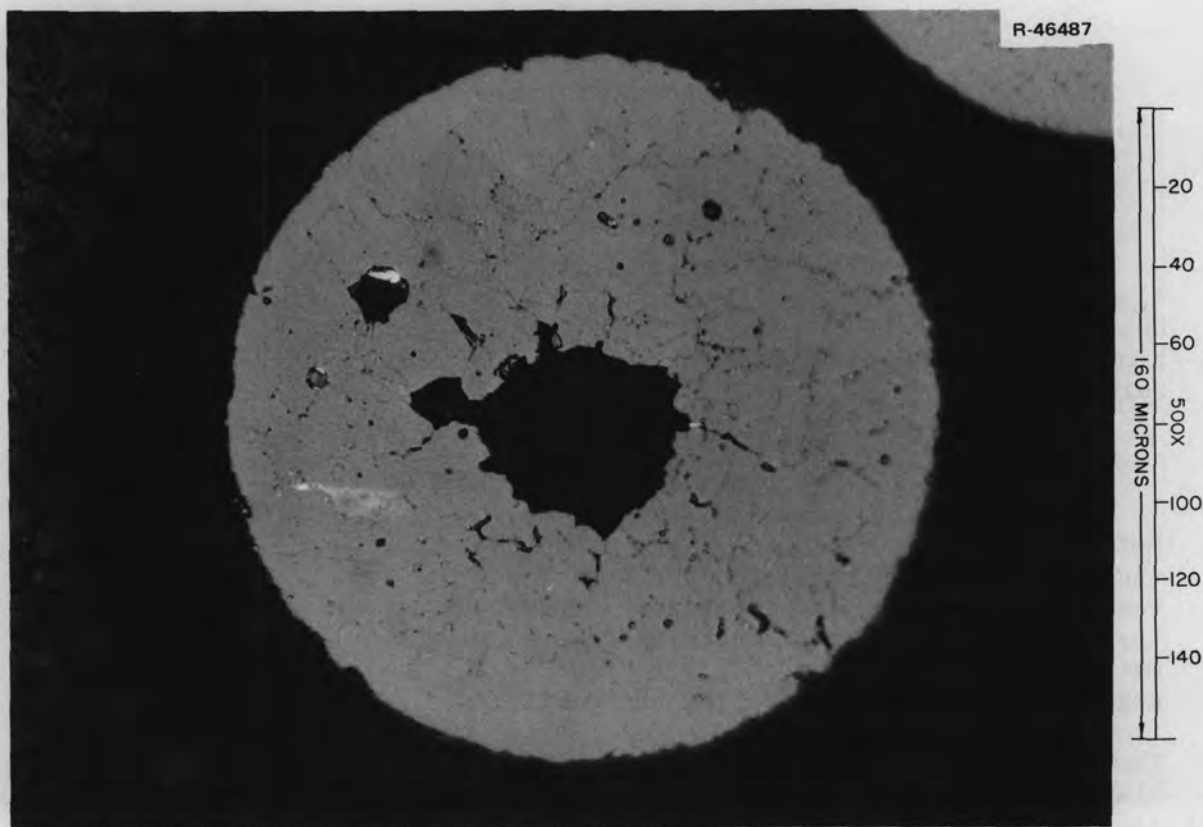


Fig. 10. Cross Section of As-Received Microsphere of SN370/376 Fuel. The large, single void is typical of a large fraction of this fuel.

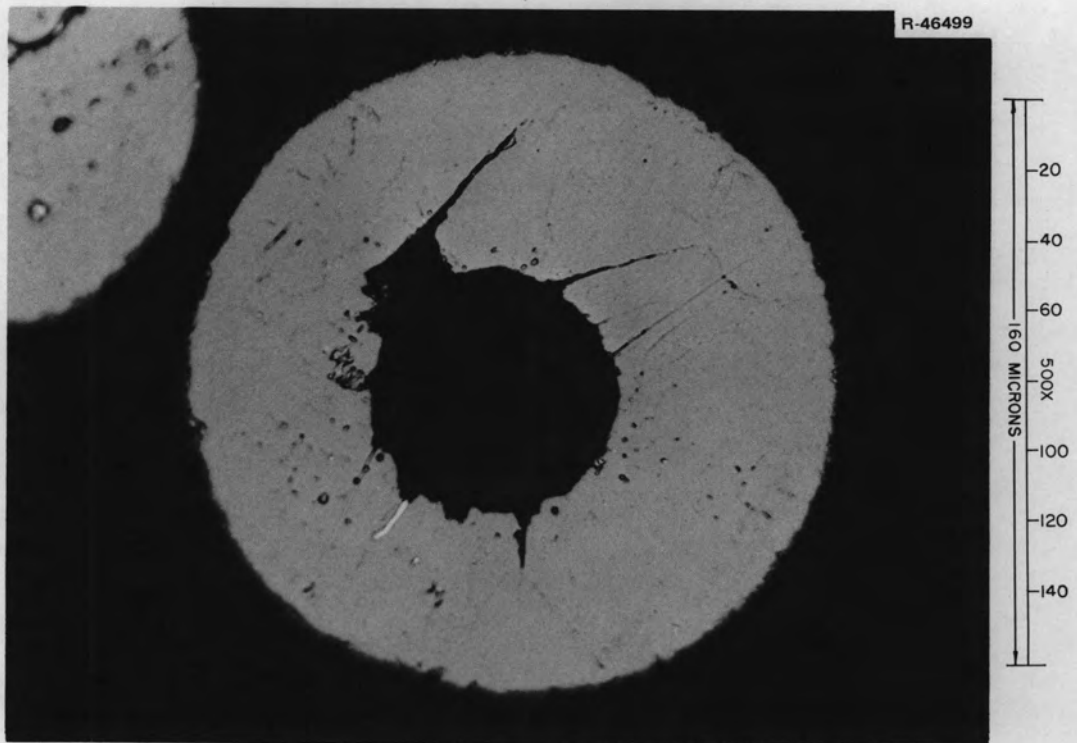


Fig. 11. A Large, Single Central Void Also Was Characteristic of a Significant Fraction of the As-Received Dart I Fuel.

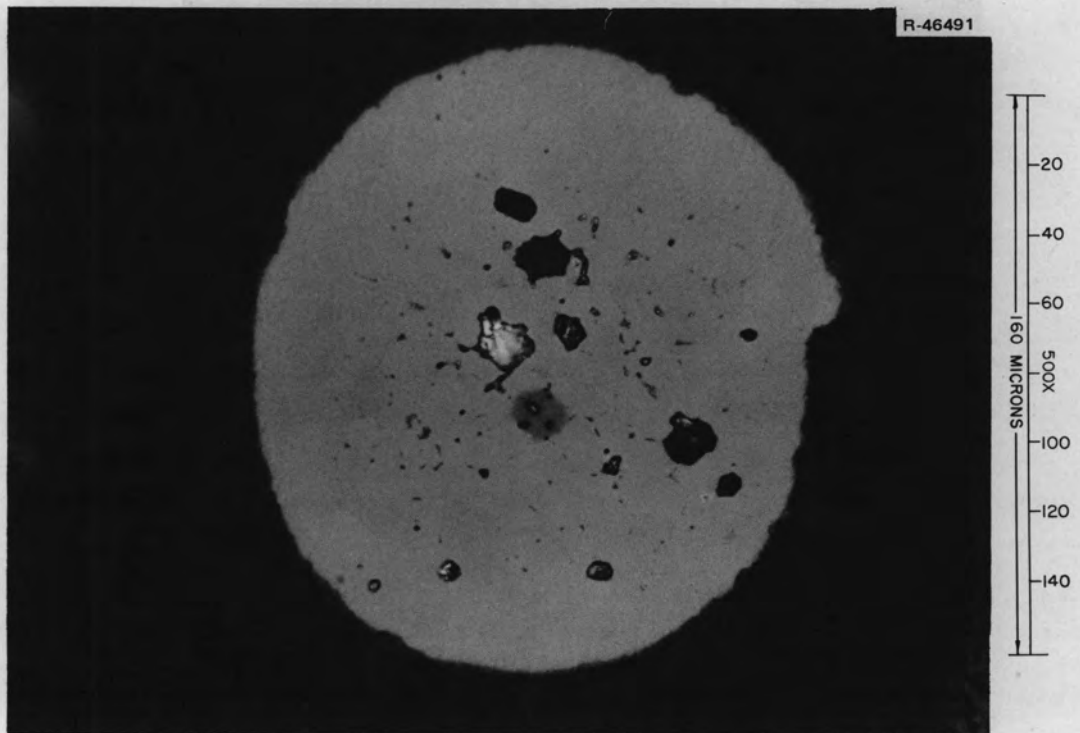


Fig. 12. Cross Section of As-Received Microsphere of SN370/376 Fuel. Particles with bulk densities higher than this were rare.

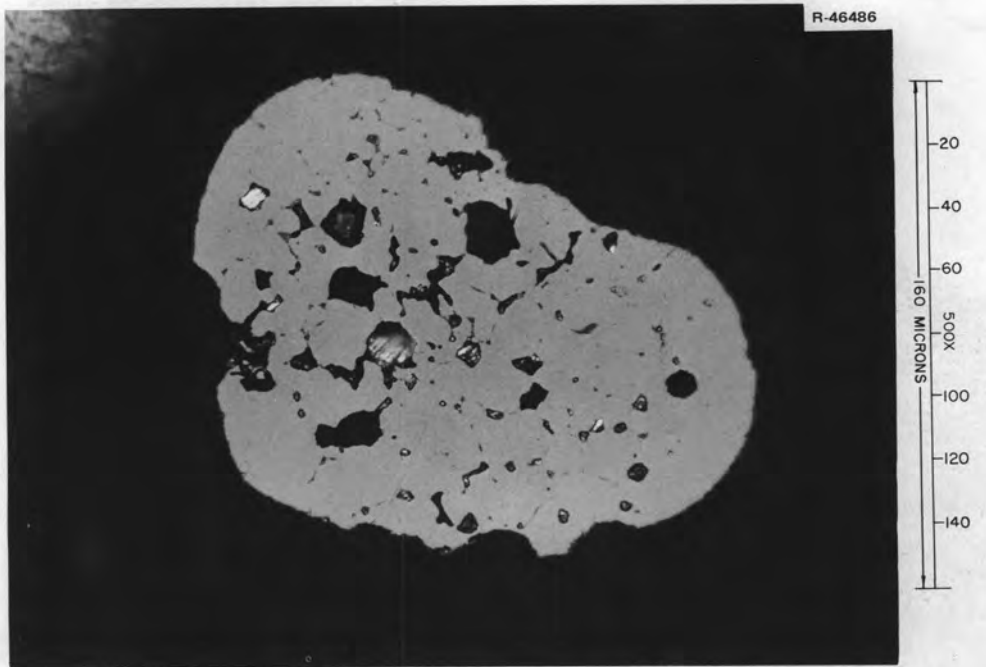


Fig. 13. A Typical Cross Section of SN370/376 Fuel in the As-Received Condition.

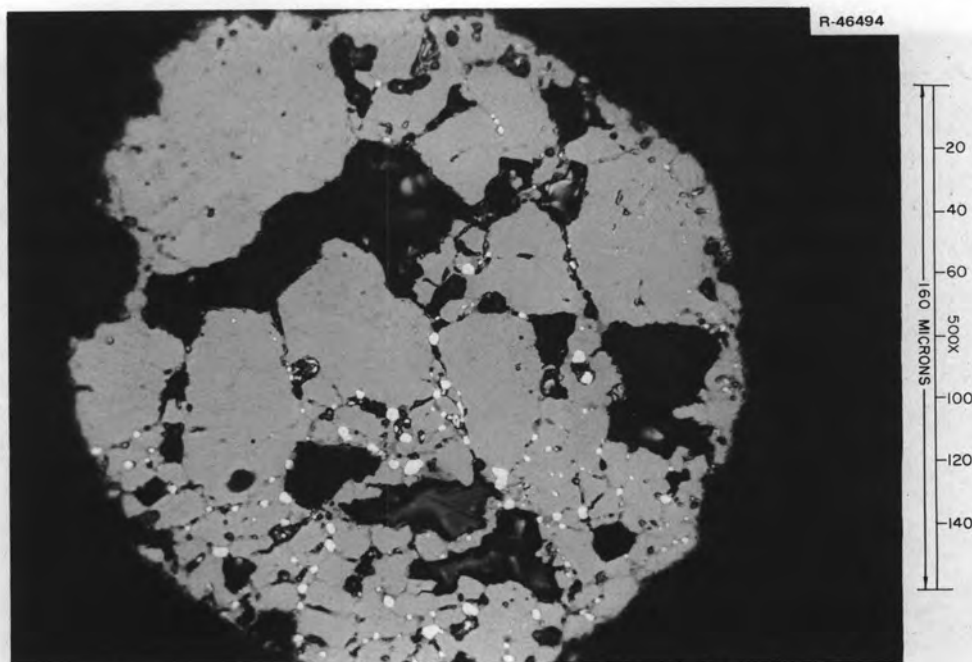


Fig. 14. Cross Section of As-Received Dart I Fuel, Typical of a Large Fraction. Note the second-phase inclusions and the weak grain boundaries.

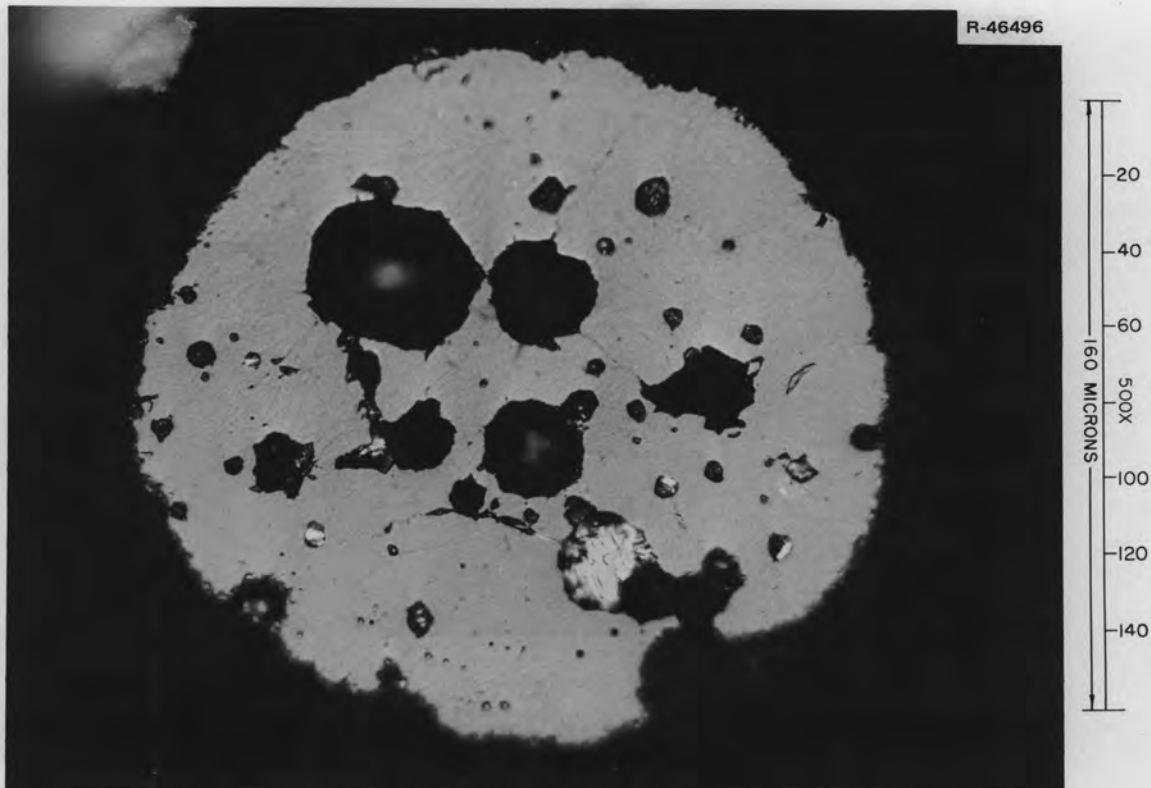


Fig. 15. A Large Fraction of the As-Received Dart I Fuel Showing Distribution of Large Spherical Voids.

In the SN370/376 fuel the formation of gas bubbles is not evident until the microspheres are heated to at least  $1100^{\circ}\text{C}$  (see Fig. 16). These gas bubbles are predominantly found in the grain boundary and are barely discernible within a grain. In the Dart I fuel, gas bubbles were not found at any temperature. An examination of photomicrographs suggests that this was due to the Dart I fuel being more porous than the SN370/376 fuel. In some instances in the SN370/376 fuel, gas bubbles were found within grains and in the grain boundaries, but did not appear in regions surrounded by large voids. At  $1300^{\circ}\text{C}$  gas bubbles within the grains became very evident in SN370/376 fuel and were found within the grain boundaries as well (see Fig. 17).

For SN370/376 fuel heated to either  $1500$  or  $1700^{\circ}\text{C}$ , there was no evidence of gas bubbles. Apparently the time of the experiment was sufficient for all the gas bubbles to be swept out of the particles. Figure 18 shows a typical cross section of a microsphere heated to  $1700^{\circ}\text{C}$  in which there is some indication that a rapid temperature excursion can cause fragmentation. Typical cross sections of some fragmented particles are shown in Figs. 19 and 20. Some fragmentation occurred, but most of the microspheres remained intact.

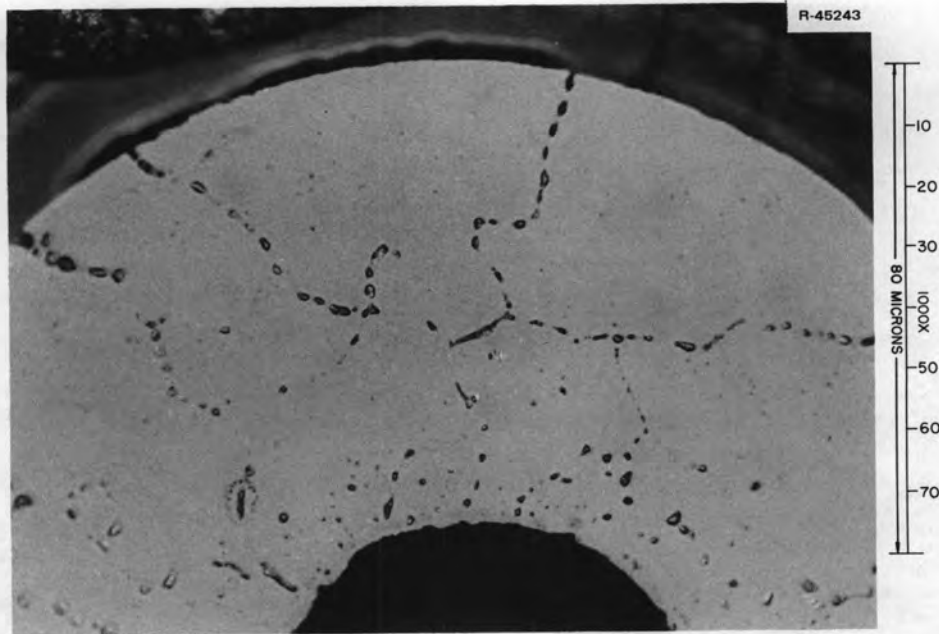


Fig. 16. Cross Section of SN370/376 Fuel (177- to 210- $\mu$  dia) Heat-Treated to 1100°C. Well-defined gas bubbles exist in the grain boundaries. At temperatures less than 1100°C gas bubbles are not readily discernible.

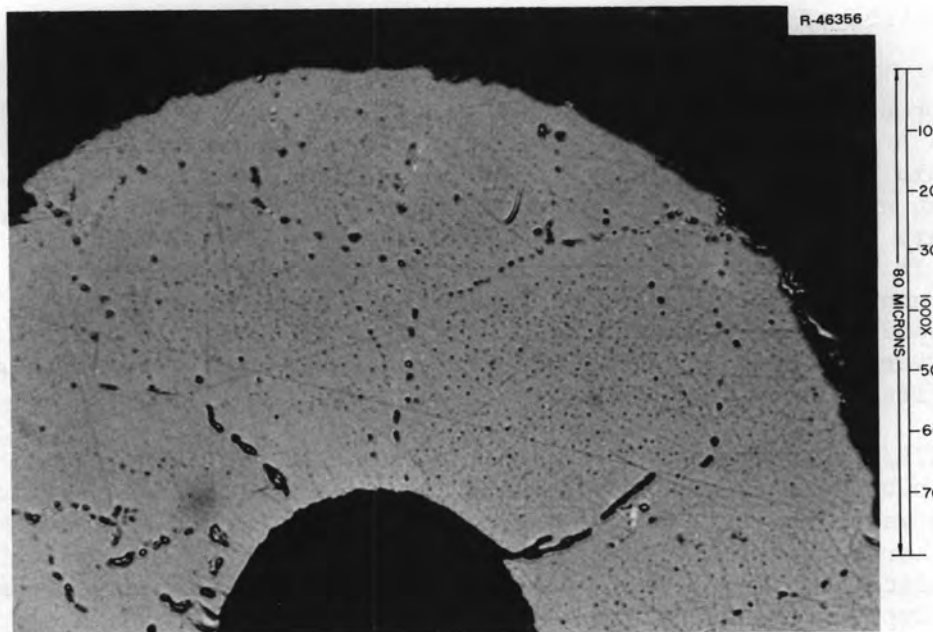


Fig. 17. SN370/376 Fuel Heat-Treated at 1300°C in Which Gas Bubbles Are Well Defined in Both the Grain Boundary and Within the Grain.

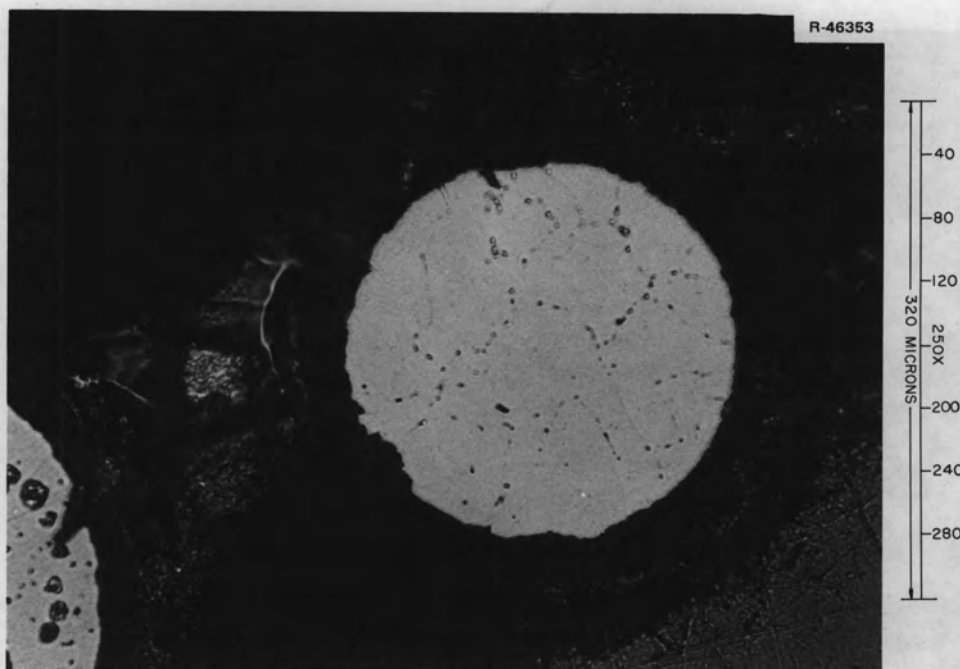


Fig. 18. A Typical Cross Section of a Microsphere Heated to 1700°C. Gas bubbles are not apparent.

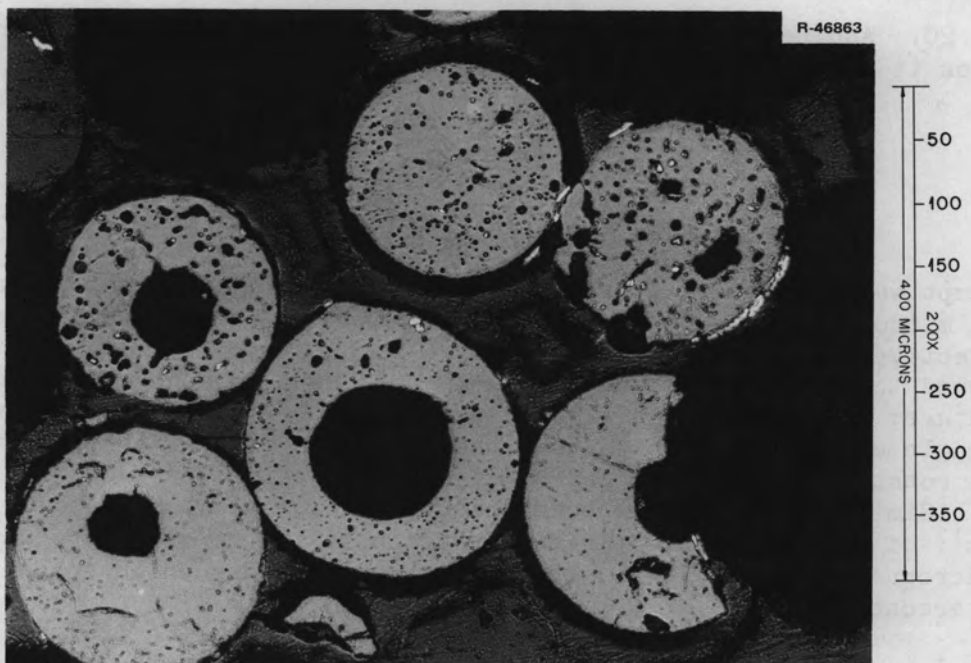


Fig. 19. Cross Section of Dart I Fuel Microsphere Heated to 1700°C. Some fragmentation has occurred, but most of the microspheres remain intact.

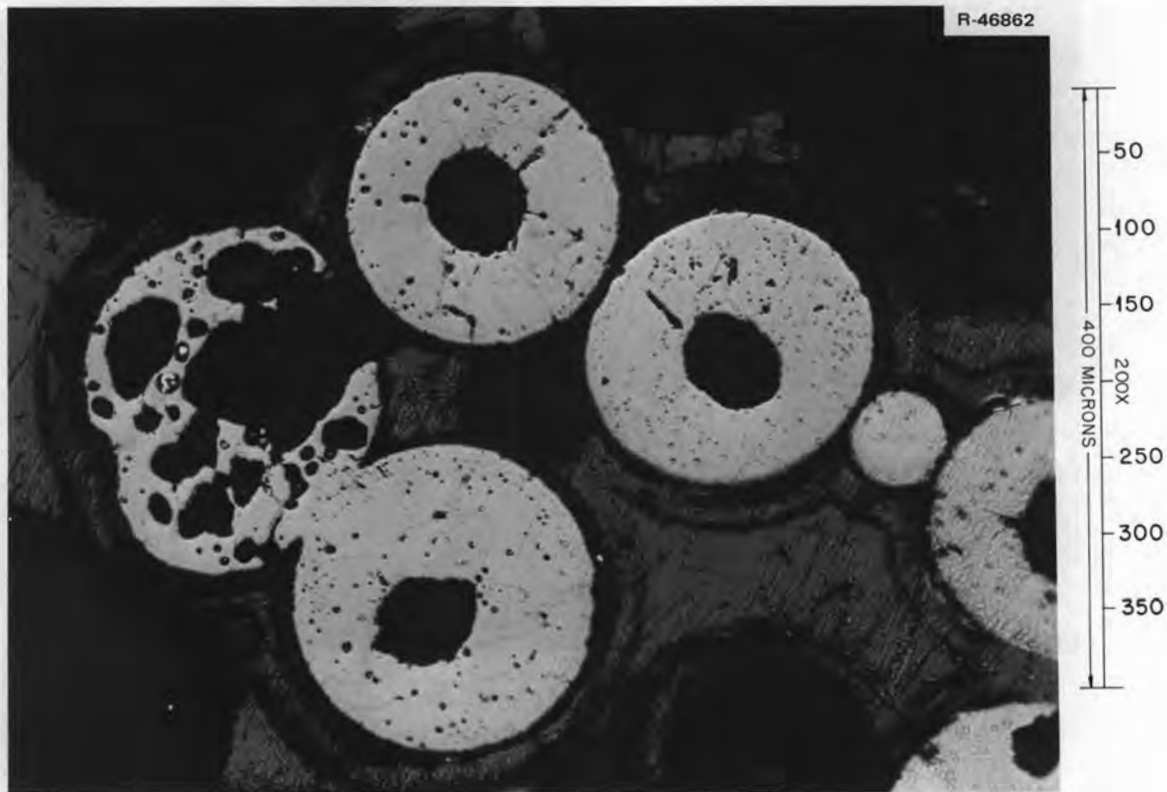


Fig. 20. Another Cross Section of Particle Heated to 1700°C. Fragmentation is also evident, but most remain intact.

## DISCUSSION

### Release Parameters for Steady-State Experiments

An attempt was made to calculate diffusion coefficients of helium in  $^{238}\text{PuO}_2$  microspheres using the geometric radius of the microsphere as the effective radius. However, diffusion coefficients thus calculated were found to be a function of the radius of the microsphere at constant temperature; the values of diffusion parameter  $D' = D/a^2$  correlate well on a single curve. This shows that the effective size of a releasing unit is constant and is independent of the size of the  $^{238}\text{PuO}_2$  microsphere. Similar effects have been observed in  $\text{UO}_2$  (ref. 11) and  $\text{Cm}_2\text{O}_3$  pellets<sup>12</sup> of various sizes. This conclusion is further supported by the photomicrographs (Figs. 10-20) showing extensive pores which apparently are interconnected.

The steady-state diffusion parameter results plotted in Fig. 3 suggest a mechanism whereby helium diffuses in  $^{238}\text{PuO}_2$  by two simultaneous processes, one process fitted by the equation

$$D/r^2 = 1.9 \times 10^{-5} \exp(-17,900/RT) \quad (10)$$

which is predominant below 1100°C, and the other process fitted by the equation

$$D/r^2 = 5.76 \times 10^5 \exp(-86,800/RT) \quad (11)$$

which is predominant above 1100°C.

Matzke<sup>5</sup> observed that radon diffuses in  $\alpha$ -Al<sub>2</sub>O<sub>3</sub> similarly by two processes having activation energies of 21 and 80 to 85 kcal/mole as compared with 17.9 and 77 kcal/mole for helium in <sup>238</sup>PuO<sub>2</sub>. He compares the activation energy for the high-temperature process (80 to 85 kcal/mole) with the activation energy for the self-diffusion of Al in Al<sub>2</sub>O<sub>3</sub> (~85 kcal/mole) and concludes that the high-temperature process is by volume diffusion. He suggests that the self-diffusion of Al in Al<sub>2</sub>O<sub>3</sub> is controlling.

The migration of helium in UO<sub>2</sub> has been studied by Gulden<sup>6</sup> by observation of bubbles using an electron microscope. She concludes that at temperatures (isothermal) of 1400 to 1500°C the helium migrates randomly as bubbles by a volume diffusion process controlled by the diffusion of uranium in the UO<sub>2</sub>. The activation energy for bubble migration was 130 ± 25 kcal/mole. Gulden,<sup>6</sup> Matzke,<sup>5</sup> and others<sup>2,3</sup> conclude that the rare gases diffuse in ionic metal oxides by diffusion of point defects which are occupied by the rare gas.

Helium, due to its exceedingly low solubility,<sup>13</sup> is believed to exist in <sup>238</sup>PuO<sub>2</sub> in point defects whose concentration and mobility would determine the diffusion of helium; consequently those factors which would determine the concentration of point defects are of interest. Kingery<sup>14</sup> discusses the enhanced low-temperature diffusion (extrinsic) and the high-temperature diffusion (intrinsic) and gives examples of several ionic solids which exhibit a knee in the plot of diffusion coefficient as a function of temperature. In all cases he attributes the extrinsic diffusion to the presence of temperature-independent cationic or anionic vacancies. Temperature-independent vacancies are produced by divalent ions in tri- or tetravalent compounds (cation vacancies) or anion vacancies in the case of ZrO<sub>2</sub> to which CaO has been added. The activation energies reported for extrinsic diffusion are low (25 to 35 kcal/mole), since only the energy to mobilize, instead of the energy to create, a vacancy is required.

Two other means by which point defects may be created in <sup>238</sup>PuO<sub>2</sub> are anionic vacancies caused by a slight reduction of the <sup>238</sup>PuO<sub>2</sub> and radiation-produced Frenkel defects; PuO<sub>2-x</sub> retains its fluorite structure down to PuO<sub>1.61</sub>.<sup>15</sup> Wechsler<sup>16</sup> has discussed the enhancement of diffusion by radiation damage.

Although at present sufficient information has not been presented to establish conclusively the processes controlling the diffusion of helium in PuO<sub>2</sub> at steady state, the information available suggests that, at high temperature, helium diffuses as bubbles by a vacancy diffusion process

controlled by the diffusion of Pu ion in  $\text{PuO}_2$ . At low temperatures, the presence of vacancies not created by thermal activation allows a low activation energy process to predominate in the helium migration. No choice among the possible mechanisms which would produce the vacancies can be made at this time.

### Transient-Heating Experiments

The results of the transient-heating experiments cannot be reconciled with a classical diffusion mechanism in spite of the usefulness of the diffusion equations in data correlation. Three major difficulties are evident:

1. At the final temperatures below  $1300^\circ\text{C}$ , there is a significant delay between the time that the peak temperature is attained and the time at which the peak release rate occurs (see Fig. 4 and Table 3).
2. The effective  $D'$  values calculated from the transient-heating experimental results are 2 to 3 orders of magnitude above those obtained in the steady-state experiments at the same temperature.
3.  $D'$  values appear to be sensitive to heating rate (see Table 3).

One may postulate that these effects arise due to the role of bubbles in helium release during transient heating. The bubbles may nucleate at a temperature-dependent rate, which is significantly slower than the heatup rate below  $1300^\circ\text{C}$ . Subsequent bubble motion could be influenced by temperature gradients arising during heating, as well as by the size of bubbles attained. These effects could be completely different from those obtained during steady-state release. It is also possible that the enhanced release rates under transient conditions result from a high number of radiation-induced effects which are present at ambient temperatures at the start of the experiments, and might not be annealed during the short time at elevated temperatures.

### CONCLUSIONS

Experimental studies of helium release from plasma-melted  $^{238}\text{PuO}_2$  microspheres revealed the following characteristics.

Helium release under steady-state conditions over the range  $100$  to  $1300^\circ\text{C}$  can be correlated in terms of a diffusion model with a temperature-dependent diffusion release parameter,  $D'$ , which was independent of microsphere size. A reasonable mechanistic model can be postulated to explain the observed behavior.

With transient heating from ambient to a constant final temperature ranging from  $900$  to  $1900^\circ\text{C}$ , with heatup times of  $2$  to  $5$  min:

1. Helium release appears to be complete at final temperatures of 1300°C and above. The time for complete release decreases from 10 to 20 min at 1300°C to less than 2 min at 1900°C.
2. Helium release can be correlated in terms of a diffusion model with two temperature-dependent parameters, an incubation time  $t_0$ , and a release parameter  $D'$ . These parameters are probably dependent on heating rate, but the present experiments were unable to define this dependence. They are independent of microsphere size.
3. At the heating rates, final temperatures, and initial helium inventories encountered in this study, there was negligible mechanical degradation of the microspheres during the release process.
4. The mechanism of helium release under transient conditions is unclear, but appears to differ significantly from that at steady state.

## REFERENCES

1. U. S. Atomic Energy Commission, Radioisotopes. Production and Development of Large-Scale Uses, USAEC Rpt. Wash-1095 (May 1968).
2. R. M. Carroll, Fission-Product Release from Fuels, Nucl. Safety 7(1): 34-44 (Fall 1965).
3. R. M. Carroll, Fission-Gas Behavior in Fuels, Nucl. Safety 10(3): 210-16 (May-June 1969).
4. Modern Concepts of Fission-Gas Release in  $UO_2$ , Nucl. Appl. 2(2): 116-80 (1966).
5. HJ. Matzke, Rare-Gas Mobility in Some Anisotropic Ceramic Oxides:  $Al_2O_3$ ,  $Cr_2O_3$ ,  $Fe_2O_3$ ,  $U_3O_8$ , J. Mater. Sci. 2: 444-56 (1967).
6. Mary Ellen Gulden, Migration of Gas Bubbles in Irradiated Uranium Dioxide, J. Nucl. Mater. 23(1): 3036 (1967).
7. H. S. Carslaw and J. C. Jaeger, Conduction of Heat in Solids, 2 ed., p. 232, Clarendon Press, Oxford, 1959.
8. P. Angelini and R. E. McHenry, Diffusion of Helium in Curium-244 Fuel Forms, Abstracts of Papers, Am. Chem. Soc., San Francisco, March 31-April 5, 1968.
9. J. Crank, The Mathematics of Diffusion, pp 147 ff, Clarendon Press, Oxford, 1956.
10. Pei Sung and J. E. Turnbaugh, Calculation of Diffusivity and Solubility with Error Analysis for Diffusion in a Sphere, J. Appl. Phys. 39: 346-47 (1968).
11. W. B. Cottrell et al., Fission Product Release from  $UO_2$ , ORNL-2935, Oak Ridge National Laboratory (September 1960).
12. P. Angelini, personal communication (June 1969).
13. Pei Sung, University of Washington, Equilibrium Solubility and Diffusivity of Helium in Single-Crystal Uranium Oxide, presented at Nuclear Division Fall Meeting of American Ceramic Society, October 6-9, 1968, Pittsburgh, Pa.
14. W. D. Kingery, Introduction to Ceramics, pp. 227-36, Wiley, New York, 1960.
15. T. D. Chikalla, et al., The Plutonium Oxygen System, HW-74802, Hanford Atomic Products Operations (1962).
16. M. S. Wechsler, Diffusion and Body-Centered Cubic Metals, pp. 291-312, American Society for Metals, Metals Park, Ohio, 1965.

ORNL-4507  
UC-33 - Propulsion Systems and  
Energy Conversion

## INTERNAL DISTRIBUTION

1-3. Central Research Library	56. Lynda Kern
4-5. ORNL - Y-12 Technical Library	57. E. Lamb
Document Reference Section	58. J. M. Leitnaker
6-25. Laboratory Records Department	59. E. L. Long, Jr.
26. Laboratory Records, ORNL R.C.	60. H. G. MacPherson
27. G. M. Adamson	61. R. W. McClung
28. P. Angelini	62. R. E. McDonald
29. P. S. Baker	63. D. L. McElroy
30. E. E. Beauchamp	64-88. R. E. McHenry
31. E. S. Bomar, Jr.	89. W. R. Martin
32. B. S. Borie, Jr.	90. A. J. Miller
33. D. T. Bourgette	91. P. Patriarca
34. G. E. Boyd	92. J. W. Prados
35. T. A. Butler	93. M. E. Ramsey
36. D. A. Canonico	94. R. A. Robinson
37. R. M. Carroll	95. W. C. Robinson, Jr.
38. F. N. Case	96. A. F. Rupp
39. N. C. Cole	97. A. C. Schaffhauser
40. K. V. Cook	98. R. W. Schaich
41. J. E. Cunningham	99. J. L. Scott
42. J. H. DeVan	100. M. J. Skinner
43. J. R. DiStefano	101. G. M. Slaughter
44. R. G. Donnelly	102. R. L. Stephenson
45. W. S. Ernst, Jr.	103. D. A. Sundberg
46. J. H. Frye, Jr.	104. R. W. Swindeman
47. J. H. Gillette	105-151. D. B. Trauger
48. R. W. Gunkel	152. M. S. Wechsler
49. W. O. Harms	153. R. L. Wagner
50. R. F. Hibbs	154. A. M. Weinberg
51-54. Meredith Hill	155. J. R. Weir
55. H. Inouye	

## EXTERNAL DISTRIBUTION

156. Robert Anderson, Sanders Nuclear, Nashua, New Hampshire  
 157. Robert Andelin, Donald W. Douglas, Richland  
 158. A. J. Arker, General Electric, Valley Forge, Pennsylvania  
 159. N. F. Barr, Office of General Manager, AEC, Washington, D.C.  
 160. H. Bloomfield, NASA/Lewis, Cleveland, Ohio  
 161. Donald Cole, AEC-DID, Washington, D.C.  
 162. D. C. Davis, Laboratory and University Division, AEC, ORO  
 163. Paul Dick, Isotopes, Inc., Westwood, New Jersey  
 164. G. K. Dicker, AEC-SNS, Washington, D.C.  
 165. T. J. Dobry, AEC-SNS, Washington, D.C.  
 166. Jerry English, Mound, Miamisburg, Ohio

167. Donald Evans, TRW, Redondo Beach California
168. Wayne Fisher, AEC-ALO, Albuquerque, New Mexico
- 169-176. E. E. Fowler, AEC-DID, Washington, D.C.
177. J. E. Fox, AEC-RDT, Washington, D.C.
178. Michael Gaitanis, AEC-SNS, Washington, D.C.
179. Neal Goldenberg, AEC-SNS, Washington, D.C.
180. Joseph Griffo, AEC-SNS, Washington, D.C.
181. Frank Haines, AEC-DID, Washington, D.C.
182. J. E. Hansen, PNL, Richland
183. D. G. Harvey, Sanders Nuclear, Nashua, New Hampshire
184. Read Holland, Sandia Corporation, Albuquerque, New Mexico
185. Dean Houston, Battelle Memorial Institute, Columbus, Ohio
186. L. C. Ianniello, AEC-RD, Washington, D.C.
187. J. W. Irvine, 6-426, MIT, Cambridge, Massachusetts
188. T. R. Jones, AEC-RD, Washington, D.C.
189. A. Kasberg, NUMEC, Apollo, Pennsylvania
190. W. K. Kern, AEC-SNS, Washington, D.C.
191. Carl Kershner, Mound, Miamisburg, Ohio
192. Chang-Kyo Kim, WANL, Pittsburgh, Pennsylvania
193. Harry Kling, Hittman Assoc., Columbia, Maryland
194. Bernard Leefer, NASA/HQ, Washington, D.C.
195. P. E. McCourt, Atomics International, North American Rockwell Corporation, P. O. Box 309, Canoga Park, California 91304
196. Barbara Mueller, Los Alamos Scientific Laboratory, Los Alamos, New Mexico
197. R. Mulford, Los Alamos Scientific Laboratory, Los Alamos, New Mexico
198. C. Northrup, Sandia Corporation, Albuquerque, New Mexico
199. P. O'Riordan, AEC-SNS, Washington, D.C.
200. Charles Peacock, NASA/MSFC, Houston, Texas
201. J. A. Powers, AEC-SNS, Washington, D.C.
202. G. M. Prok, NASA/Lewis, Cleveland, Ohio
203. G. Rausa, Weiner Associates, Baltimore, Maryland
204. Sol Rosen, AEC-RDT, Washington, D.C.
205. Mel Shupe, Los Alamos Scientific Laboratory, Los Alamos, New Mexico
206. Tom Smith, Donald W. Douglas, Richland
207. Neal Strazza, Isotopes, Inc., Westwood, New Jersey
208. Vince TeSantis, General Electric, Valley Forge, Pennsylvania
209. J. A. Swartout, Union Carbide Corporation, New York
210. J. R. Thompson, Battelle Memorial Institute, Columbus, Ohio
211. M. Tobin, Westinghouse Astronuclear Nuclear Laboratory, Pittsburgh, Pennsylvania
212. Leonard Topper, AEC-SNS, Washington, D.C.
- 213-217. Vincent Truscello, Jet Propulsion Laboratory, California Institute of Technology, 4800 Oak Grove Drive, Pasadena, California 91103
218. M. E. McClain, Jr., Nuclear Research Center, Georgia Institute of Technology, Atlanta, Georgia 30332
219. Ruth Weltman, NASA/Lewis, Cleveland, Ohio
220. David Williams, Sandia Corporation, Albuquerque, New Mexico
221. Ronald Zielinski, Mound, Miamisburg, Ohio

- 222. R. B. Martin, Laboratory and University Division, AEC, ORO
- 223. J. N. Maddox, AEC, Washington, D.C.
- 224. H. M. Roth, Laboratory and University Division, AEC, ORO
- 225-421. Given distribution as shown in TID-4500 under Propulsion Systems and Energy Conversion category (25 copies -CFSTI)